SIAM J. APPL., MATH.
Vol. 43, No. 4, August 1983

0036-1399/83/4304-0022 $01.25/0

FAST SEISMIC RAY TRACING*

H. B. KELLER† AND D. J. PEROZZI‡

Dedicated to Joseph Keller in honor of all his contributions

Abstract. New methods for the fast, accurate and efficient calculation of large classes of seismic rays joining two points $\mathbf{x}_S$ and $\mathbf{x}_R$ in very general two-dimensional configurations are presented. The medium is piecewise homogeneous with arbitrary interfaces separating regions of different elastic properties (i.e., differing wave speeds c_P and c_S). In general there are 2^{N+1} rays joining $\mathbf{x}_S$ to $\mathbf{x}_R$ while making contact with N interfaces. Our methods find essentially all such rays for a given N by using continuation or homotopy methods on the wave speeds to solve the ray equations determined by Snell's law. In addition travel times, ray amplitudes and caustic locations are obtained. When several receiver positions $\mathbf{x}_R^{(j)}$ are to be included, as in a gather, our techniques easily yield all the rays for the entire gather by employing continuation in the receiver location. The applications, mainly to geophysical inverse problems, are reported elsewhere.

1. Introduction. In this paper we present new fast, efficient and accurate methods for determining large classes of seismic rays joining two arbitrary points, $\mathbf{x}_S$ and $\mathbf{x}_R$, in very general two-dimensional configurations. We allow arbitrary geological interfaces and free surfaces separating or bounding various regions of different homogeneous isotropic elastic material, i.e. differing *constant* wave speeds c_P and c_S. In general we expect that there can be 2^{N+1} distinct seismic rays joining $\mathbf{x}_S$ and $\mathbf{x}_R$ if each ray makes contact with N interfaces or bounding surfaces. This is because on contact with an interface a seismic wave (compressive or shear) may change type or it may not. Our new procedures easily determine all or most such rays for a given N. Travel time and amplitude variation along each ray are determined. Phase shifts along the rays are also determined since the occurrence of every caustic on any ray is detected and the phase shifts at an interface are calculated. From this data, compiled for some set of integers, say $N = 1, 2, \cdots, N_{\max}$, we can construct very realistic artificial seismograms.

Of course the basic goals of this work are to solve various geophysical inverse problems. We have already used our new techniques to determine source locations, media speeds and interface locations in test problems, see Perozzi [5]. These applications will be reported elsewhere.

In § 2 we formulate the ray problem for the general piecewise constant plane configuration. It reduces to systems of coupled nonlinear equations—Snell's law—since the rays are piecewise linear. We also introduce the notion of the "signature" of a ray which is a useful device for labelling rays. It is of help in devising simple computer codes for solving the ray problem.

In § 3 we describe the solution procedures that we employ: Newton's method and continuation in speeds and receiver location. A particular continuation or homotopy procedure is devised to get the first ray with a given number, N, of interface contacts.

In § 4 we discuss briefly the computation of travel time, amplitude variation and phase. A worked out example is contained in § 5.

The current work does not include the computation of diffracted rays. However using the theory developed by J. B. Keller [3] such rays could be included. The

* Received by the editors November 23, 1982. This research was supported by the U.S. Geological Survey under contract 14-08-0001-16777 and by the Department of Energy (Office of Basic Energy Sciences) under contract DE-AS03-76SF 00767.

† Applied Mathematics, California Institute of Technology, Pasadena, California 91125.

‡ Sohio Petroleum Company, Houston, Texas 77210.

beginnings of the practical determination of such contributions are included in Perozzi [5] where some diffracted rays and their travel times are determined. To include amplitude calculations we must employ the methods of J. B. Keller and this will be done in the future.

2. Formulation. The earth structure is modelled by piecewise constant regions of arbitrary shape. The interfaces between regions as well as the free surface of the earth are assumed to be smooth curves, say represented by the formulas[1]

$$y = f_i(x), \qquad i = 0, 1, 2, \cdots, M. \tag{2.1}$$

We shall adopt the convention that $i = 0$ represents the free surface of the earth; thus we are only concerned with the domain $y \leqq f_0(x)$. At the present we do not consider intersecting interfaces (i.e. as at corners of a region). This is merely a simplifying assumption to aid in understanding our general methods; the intersection of interfaces can be included with some slight additional complications. So our configuration consists of "layers" but the interfaces need not be parallel nor simple geometric shapes; see Figs. 1 and 2.

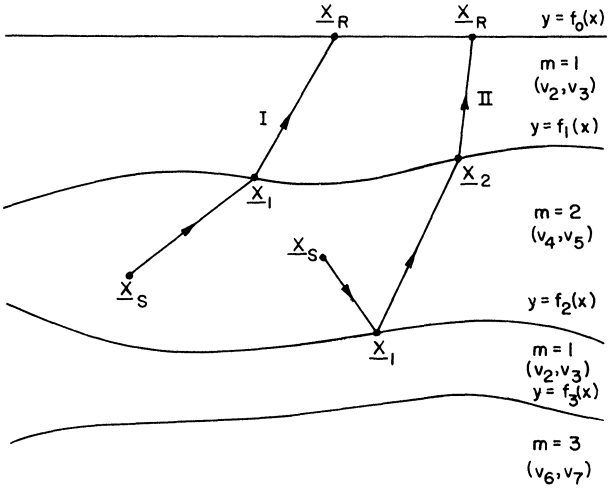

FIG. 1. *Schematic diagram of a four layered medium with arbitrary interfaces, $y = f_i(x)$, and wave speeds: $c_P = v_{2m}$ and $c_S = v_{2m+1}$ in medium m. Rays of two different classes are shown.*

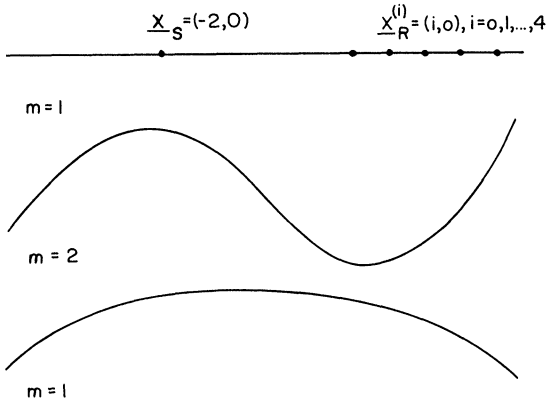

FIG. 2. *Source and gather locations for the computational example with three layers.*

[1] Our techniques easily include other representations of the interfaces such as $x = g_i(y)$ or the parametric form: $x = x_i(s)$, $y = y_i(s)$.

The medium between each successive pair of interfaces is assumed homogeneous, isotropic and perfectly elastic. Thus at most two kinds of signals can propagate in such media, compressive with speed c_P and shear with speed c_S. These speeds of course differ in different media. The rays however must all be straight line segments in each region—thus no differential equations need be solved. A ray is determined geometrically by knowing the initial or "source" point, $\mathbf{x}_S$, the final or "receiver" point, $\mathbf{x}_R$, and each contact point or node, $\mathbf{x}_k$, at which the ray meets an interface. Further on each segment $[\mathbf{x}_{k-1}, \mathbf{x}_k]$ its type of propagation must be known and this is equivalent to specifying the speed, c_P or c_S, in the medium containing that segment. At the contact points Snell's law must hold and this serves to determine the nodes as we now show.

Let the speed on the segment $[\mathbf{x}_{k-1}, \mathbf{x}_k]$ be denoted by v_k for each $k = 1, 2, \cdots, N$. Let a tangent vector to the interface at each node, $\mathbf{x}_k$, be denoted by $\boldsymbol{\tau}_k$. Then Snell's law in its most general (plane) form requires that

$$v_{k+1}\left(\boldsymbol{\tau}_k \cdot \frac{\mathbf{x}_k - \mathbf{x}_{k-1}}{|\mathbf{x}_k - \mathbf{x}_{k-1}|}\right) = v_k\left(\boldsymbol{\tau}_k \cdot \frac{\mathbf{x}_{k+1} - \mathbf{x}_k}{|\mathbf{x}_{k+1} - \mathbf{x}_k|}\right). \tag{2.2}$$

Here we have used the vector notation $\mathbf{x}_k \equiv (x_k, y_k)$ and $(\boldsymbol{\tau} \cdot \mathbf{x})$ represents the usual scalar product of vectors. From the interface representation (2.1) it follows that when $\mathbf{x}_k$ is on the interface i_k, say:

$$\mathbf{x}_k \equiv (x_k, y_k) = (x_k, f_{i_k}(x_k)). \tag{2.3a}$$

Also a tangent to the i_kth interface at $\mathbf{x}_k$ is given, with $f'(x) \equiv df(x)/dx$, by:

$$\boldsymbol{\tau}_k = (1, f'_{i_k}(x_k)). \tag{2.3b}$$

Using (2.3) in (2.2) we get

$$\begin{aligned}\phi_k \equiv v_{k+1} &\frac{(x_k - x_{k-1}) + f'_{i_k}(x_k)(f_{i_k}(x_k) - f_{i_{k-1}}(x_{k-1}))}{[(x_k - x_{k-1})^2 + (f_{i_k}(x_k) - f_{ik-1}(x_{k-1}))^2]^{1/2}} \\ -v_k &\frac{(x_{k+1} - x_k) + f'_{i_k}(x_k)(f_{i_{k+1}}(x_{k+1}) - f_{i_k}(x_k))}{[(x_{k+1} - x_k)^2 + (f_{i_{k+1}}(x_{k+1}) - f_{i_k}(x_k))^2]^{1/2}} = 0.\end{aligned} \tag{2.4}$$

The relations (2.4) must hold at each interface, say for $k = 1, 2, \cdots, N$, on a ray meeting N interfaces between $\mathbf{x}_S$ and $\mathbf{x}_R$. Of course since the source location, $\mathbf{x}_S$, and the receiver location, $\mathbf{x}_R$, are assumed known there are only N unknowns in (2.4), the *scalars*: $x_1, x_2, \cdots, x_N$. For $k = 1$ and $k = N$ in (2.4) we must use

$$\begin{aligned} &\text{a)} \quad \mathbf{x}_0 = (x_0, y_0) = (x_0, f_{i_0}(x_0)) = (x_S, y_S), \\ &\text{b)} \quad \mathbf{x}_{N+1} = (x_{N+1}, y_{N+1}) = (x_{N+1}, f_{i_{N+1}}(x_{N+1})) = (x_R, y_R). \end{aligned} \tag{2.5}$$

The notation $f_{i_0}(x_0)$ and $f_{i_{N+1}}(x_{N+1})$ may be meaningless if as is frequently the case, $\mathbf{x}_S$ or $\mathbf{x}_R$ does not lie on an interface or free surface. But (2.5) eliminates all such difficulties. After using (2.5) in (2.4) there remain N nonlinear equations in N unknowns. If we introduce the vectors

$$X \equiv (x_1, x_2, \cdots, x_N)^T, \quad V \equiv (v_1, v_2, \cdots, v_{N+1})^T, \quad \Phi(X, V) \equiv (\phi_1, \phi_2, \cdots, \phi_N)^T, \tag{2.6}$$

then our system can be written as

$$\Phi(X, V) = 0. \tag{2.7}$$

2.1 Ray signatures, classes and propagation types. To use the above formulation we must specify on each ray to be computed the ray speed intended on each of its segments $[\mathbf{x}_{k-1}, \mathbf{x}_k]$ and the appropriate interface formula at each of its nodes, $\mathbf{x}_k$. To do this we label each different material with an integer, m, say. Then the speeds in material m are labelled as

$$c_{P,m} \equiv v_{2m}, \qquad c_{S,m} \equiv v_{2m+1}, \qquad m = 1, 2, \cdots, M. \tag{2.8}$$

Now, given $\mathbf{x}_S$ and $\mathbf{x}_R$, a ray can be classified by listing sequentially its speed on the first segment, the number of its first interface contact, etc., terminating with the speed on its final segment. This listing we call a *ray signature* and it is equivalent to listing in order the subscripts $j = 2m$ or $j = 2m+1$ for (2.8) and i for (2.1). Thus a ray signature is specified by giving an ordered set of $2N+1$ integers:

$$[j_1, i_1; j_2, i_2; \cdots; j_N, i_N; j_{N+1}]. \tag{2.9}$$

All such rays with fixed $i_1, \cdots, i_N$ form a *class* of rays with N interior nodes joining $\mathbf{x}_S$ and $\mathbf{x}_R$. There are generally 2^{N+1} rays in such a class, each being of a different *propagation type.*

Let us give some simple examples. In Fig. 1 a sketch of four layers is indicated, the first and third composed of the same material. Two different *classes* of rays are indicated: one class with one internal node called I and one class with two internal nodes called II. All possible signatures are given as follows:

(2.10)

Rays of class I:		*Rays of class* II:	
1. [4, 2; 2]	[P, P]	1. [4, 3; 4, 2; 2]	[P; P; P]
2. [4, 2; 3]	[P; S]	2. [4, 3; 4, 2; 3]	[P; P; S]
3. [5, 2; 2]	[S; P]	3. [4, 3; 5, 2; 2]	[P; S; P]
4. [5, 2; 3]	[S; S]	4. [4, 3; 5, 2; 3]	[P; S; S]
		5. [5, 3; 4, 2; 2]	[S; P; P]
		6. [5, 3; 4, 2; 3]	[S; P; S]
		7. [5, 3; 5, 2; 2]	[S; S; P]
		8. [5, 3; 5, 2; 3]	[S; S; S]

We have also listed next to each ray signature the sequence of *propagation types* represented by each such ray. This is redundant information since it can be obtained from the signature by simply observing the parity of the speed indices. But we find it useful to sometimes display the simpler propagation type signature as well.

3. Solution procedures. To solve (2.7) we employ Newton's method and continuation procedures. Specifically if we have an approximation, say X^ν, to the values X of the node abscissae, then an improved value is given by

$$X^{\nu+1} = X^\nu + \delta X^\nu, \tag{3.1a}$$

where

$$A^\nu \delta X^\nu = -\Phi^\nu. \tag{3.1b}$$

Here we have used

$$X^\nu \equiv (x_1^\nu, x_2^\nu, \cdots, x_N^\nu), \quad \Phi^\nu \equiv \Phi(X^\nu, V), \quad A^\nu \equiv A(X^\nu, V) \tag{3.2}$$

where $A(X, V)$ is the Jacobian matrix:

$$A(X, V) \equiv \frac{\partial \Phi(X, V)}{\partial X}. \tag{3.3a}$$

From (2.4)–(2.6) we find that A is an $N \times N$ tridiagonal matrix, say $A \equiv [b_k, a_k, c_k]$, where

$$b_k \equiv \frac{\partial \phi_k}{\partial x_{k-1}}, \quad a_k \equiv \frac{\partial \phi_k}{\partial x_k}, \quad c_k \equiv \frac{\partial \phi_k}{\partial x_{k+1}}. \tag{3.3b}$$

Specifically the components are:

$$\begin{aligned} a_k &= \frac{v_{k+1}}{D_k}\left[1 + y_k'' \Delta y_k + (y_k')^2 - \left(\frac{\Delta x_k + y_k' \Delta y_k}{D_k}\right)^2\right] \\ &\quad + \frac{v_k}{D_{k+1}}\left[1 - y_k'' \Delta y_{k+1} + (y_k')^2 - \left(\frac{\Delta x_{k+1} + y_k' \Delta y_{k+1}}{D_{k+1}}\right)^2\right], \\ b_k &= -\frac{v_{k+1}}{D_k}\left[1 + y_{k-1}' y_k' - \left(\frac{\Delta x_k + y_{k-1}' \Delta y_k}{D_k}\right)\left(\frac{\Delta x_k + y_k' \Delta y_k}{D_k}\right)\right], \\ c_k &= -\frac{v_k}{D_{k+1}}\left[1 + y_k' y_{k+1}' - \left(\frac{\Delta x_{k+1} + y_k' \Delta y_{k+1}}{D_{k+1}}\right)\left(\frac{\Delta x_{k+1} + y_{k+1}' \Delta y_{k+1}}{D_{k+1}}\right)\right]. \end{aligned} \tag{3.3c}$$

Here we have used the notation:

$$\Delta x_j \equiv x_j - x_{j-1}, \quad \Delta y_j \equiv y_j - y_{j-1}, \quad y_j' \equiv \frac{df_{i_j}(x_j)}{dx_j}, \quad D_j \equiv [(\Delta x_j)^2 + (\Delta y_j)^2]^{1/2}. \tag{3.3d}$$

Newton's method converges quadratically when X^0 the initial guess is sufficiently close to a solution. That is we can insure

$$\|\delta X^\nu\| \leqq K \|\delta X^{\nu-1}\|^2, \qquad \nu = 1, 2, \cdots \tag{3.4}$$

if we can also insure that X^0 is close to a solution. For this purpose we use continuation techniques.

3.1. Continuation in speeds. We consider the one-parameter family of speeds

$$V(\lambda) \equiv \lambda V + (1-\lambda)\hat{V}, \qquad 0 \leqq \lambda \leqq 1. \tag{3.5}$$

Clearly $V(0) = \hat{V}$ and $V(1) = V$. So if the solution of (2.7) using the speeds (3.5) is denoted by $X(\lambda)$ it follows that $X(0)$ is the solution using speeds $\hat{V}$ and $X(1)$ is the solution using speeds V. If the solution is known for any value of λ we can use as the initial guess in Newton's method for the value $\lambda + \Delta\lambda$ the vector

$$X^0(\lambda + \Delta\lambda) = X(\lambda) + \Delta\lambda \dot{X}(\lambda). \tag{3.6}$$

This is accurate to order $\Delta\lambda^2$ if we know $\dot{X}(\lambda) \equiv dX(\lambda)/d\lambda$. This derivative is obtained from using (3.5) in (2.7) and differentiating to get, recalling (3.3a):

$$A(X(\lambda), V(\lambda))\dot{X}(\lambda) = -\frac{\partial \Phi(X(\lambda), V(\lambda))}{\partial V}[V - \hat{V}]. \tag{3.7}$$

The matrix $B \equiv \partial\Phi/\partial V$ is $N \times (N+1)$ and is bidiagonal. Specifically the kth row of $B = (b_{k,j})$ has the elements, using the notation of (3.3d),

$$
\begin{aligned}
b_{k,k} &\equiv \frac{\partial \phi_k}{\partial v_k} = -\left(\frac{\Delta x_{k+1} + y'_k \Delta y_{k+1}}{D_{k+1}}\right), \\
b_{k,k+1} &\equiv \frac{\partial \phi_k}{\partial v_{k+1}} = \left(\frac{\Delta x_k + y'_k \Delta y_k}{D_k}\right), \\
b_{k,j} &\equiv 0, \qquad j \neq k, k+1.
\end{aligned} \tag{3.8}
$$

Thus since $A(X(\lambda), V(\lambda))$ is known at λ we easily obtain $\dot{X}(\lambda)$ by solving (3.6).

As a further simplification we note that our continuation techniques are usually employed to compute all rays in a given class (see § 2.1). If these rays of different propagation types are used in an appropriate order the vectors, say V and $\hat{V}$, from two consecutive rays differ only in one component. Then, for example, we will always have, for some k:

$$V - \hat{V} = (0, \cdots, 0, v_k - \hat{v}_k, 0, \cdots, 0)^T \tag{3.9}$$

and the right-hand side of (3.7) has only two nonzero components, the $(k-1)$st and the kth. It is easy to devise an algorithm that will march through all 2^{N+1} possible velocity sequences changing only one velocity component at each step.

In at least 90% of our test cases we were able to use the above indicated continuation procedure with $\Delta\lambda = 1$. That is, in *one step* we obtain an initial guess for which Newton's method converges for the new speeds V, from (3.6) with $\lambda = 0$ and $\Delta\lambda = 1$. This procedure is so robust that our algorithm proceeds by choosing $\Delta\lambda = 1$ to start and if Newton's method does not converge in a few iterations (say 3) we then replace $\Delta\lambda$ by $\Delta\lambda/2$ and continue. An extremely efficient algorithm results.

3.2 Continuation in receiver location. For use in geophysical prospecting the ray problems of interest involve an array of receiver locations (called a "gather") (see Fig. 2). Thus it is naturally suggested to use a ray solution joining $\mathbf{x}_S$ and $\mathbf{x}_R^{(i)}$ as the initial guess to the ray joining $\mathbf{x}_S$ and $\mathbf{x}_R^{(j)}$ provided $\mathbf{x}_R^{(i)}$ and $\mathbf{x}_R^{(j)}$ are close neighbors. Our continuation procedures supply an even better technique which is simply to continue $\mathbf{x}_R^{(i)}$ into $\mathbf{x}_R^{(j)}$. Thus in place of $\mathbf{x}_{N+1} = (x_R, y_R)$ of (2.5b) we consider:

$$\mathbf{x}_{N+1}(\lambda) \equiv \lambda \mathbf{x}_R^{(j)} + (1-\lambda)\mathbf{x}_R^{(i)} = \lambda (x_R^{(j)}, y_R^{(j)}) + (1-\lambda)(x_R^{(i)}, y_R^{(i)}). \tag{3.10}$$

Here as λ traverses the interval $[0, 1]$ the final (receiver) node $\mathbf{x}_{N+1}(\lambda)$ goes from $\mathbf{x}_R^{(i)}$ to $\mathbf{x}_R^{(j)}$. Just as in § 3.1 the solution of (2.7) using (3.10) in place of (2.5b) is denoted by $X(\lambda)$. The initial estimate of the solution for $\lambda + \Delta\lambda$ is given by (3.6) but now $\dot{X}(\lambda)$ is obtained from

$$A(X(\lambda), V; \mathbf{x}_{N+1}(\lambda))\dot{X}(\lambda) = \frac{\partial \Phi(X(\lambda), V; \mathbf{x}_{N+1}(\lambda))}{\partial \mathbf{x}_{N+1}} [\mathbf{x}_R^{(j)} - \mathbf{x}_R^{(i)}]^T. \tag{3.11}$$

Here, in $A(\cdot)$ and $\Phi(\cdot)$, we have denoted the dependence on $\mathbf{x}_{N+1}$. This was suppressed before since it was irrelevant for the previous discussion. We note now that only the final component in $\Phi(\cdot)$, called $\phi_N(\cdot)$ in (2.6), involves $\mathbf{x}_{N+1}$. The dependence is easily obtained by setting $k = N$ in (2.4). Thus we find that $\partial\Phi/\partial\mathbf{x}_{N+1}$ is a matrix of order $N \times 2$ and all components but those in the last row vanish. The

nonvanishing Nth row is: $(\partial\phi_N/\partial x_{N+1}, \partial\phi_N/\partial y_{N+1})$ where

$$\frac{\partial\phi_N}{\partial x_{N+1}} = -\frac{v_N}{D_{N+1}}\left[1+\left(\frac{\Delta x_{N+1}}{D_{N+1}}\right)^2 + f'_{i_N}(x_N)\frac{\Delta x_{N+1}\Delta y_{N+1}}{D^2_{N+1}}\right],$$
$$\frac{\partial\phi_N}{\partial y_{N+1}} = -\frac{v_N}{D_{N+1}}\left[f'_{i_N}(x_N)\left\{1+\left(\frac{\Delta y_{N+1}}{D_{N+1}}\right)^2\right\} + \frac{\Delta x_{N+1}\Delta y_{N+1}}{D^2_{N+1}}\right]. \tag{3.12}$$

Thus the right-hand side of (3.11) has all components zero save the last one which is:

$$\frac{\partial\phi_N}{\partial x_{N+1}}(x_R^{(j)} - x_R^{(i)}) + \frac{\partial\phi_N}{\partial y_{N+1}}(y_R^{(j)} - y_R^{(i)}). \tag{3.13}$$

In many applications the receivers are all located on a plane surface for which $y_R^{(j)} = y_R^{(i)}$ and so the above simplifies further.

3.3 First ray in a class of rays. We have shown in § 3.1 how to use continuation in speeds to compute all the rays of a given class of rays after one ray of that class has been determined. We now show a simple but powerful technique, based on speed continuation, for determining some first ray of any given class. Usually we pick the pure compressive ray type: $[P; P; \cdots; P]$, but this is not crucial. So we assume given $\mathbf{x}_S, \mathbf{x}_R$ and an appropriate signature of the first ray to be determined. Then we arbitrarily take, for example:

$$\hat{x}_k = x_S + k\left(\frac{x_R - x_S}{N+1}\right), \qquad k = 0, 1, \cdots, N+1. \tag{3.14}$$

We call the vector with these components X and with it and the signature indices, i_k, we then determine the nodes $\hat{\mathbf{x}}_k = (\hat{x}_k, f_{i_k}(\hat{x}_k))$. For $\hat{v}_1$ we take the correct value of v_1 as determined by the signature and the medium containing the segment $[\tilde{\mathbf{x}}_0, \hat{\mathbf{x}}_1]$. Then using (2.2) and the predetermined nodes $\hat{\mathbf{x}}_k$ we compute successively $\hat{v}_2, \cdots, \hat{v}_{N+1}$ to generate the speed vector $\hat{V}$. These speeds are generally unrelated to any physically reasonable materials—they may even be negative. Further the "ray" in question may pass through the same material several times with different propagation speeds $\hat{v}$ on each such segment (suggesting the term "Riemann sheeted material"). Nevertheless our procedure has generated vectors $\hat{X}$ and $\hat{V}$ such that

$$\Phi(\hat{X}, \hat{V}) = 0. \tag{3.15}$$

Now we simply use our continuation procedure of § 3.1 to determine the solution for the correct physical speeds V. The continuation for this first ray is usually somewhat slower than for the continuation between successive rays of different propagation types. But it too converges surprisingly fast. A theoretical justification for these continuation procedures in the present application is discussed in Perozzi [5].

For different geometric configurations we may employ different techniques to generate the nodes $\hat{\mathbf{x}}_k$. But the basic idea is as described above.

Other ways to determine the first ray in a class of rays are suggested by the continuation in receiver locations described in § 3.2. Obviously if a ray is known to go from $\mathbf{x}_S$ to $\hat{\mathbf{x}}_R$ where $\hat{\mathbf{x}}_R$ is close the desired $\mathbf{x}_R$ we can continue from $\hat{\mathbf{x}}_R$ to $\mathbf{x}_R$. Although this is described for use in a gather in § 3.2 we could possibly determine an initial ray by shooting. Indeed shooting is the standard way in which ray tracing is usually done, so we need not describe the technique here. Our continuation procedure coupled with Newton's method does not take much more computing per

iteration step than does shooting iterations (using Newton's method). But our procedures are much more stable than the shooting techniques and require far fewer iterations.

4. Travel time, amplitude, phase. After a ray has been determined we compute the time for a signal of the given propagation type to propagate from $\mathbf{x}_S$ to $\mathbf{x}_R$. Since v_k is the speed on the kth segment of the ray, $[\mathbf{x}_{k-1}, \mathbf{x}_k]$, the travel time is clearly

$$t = \sum_{k=1}^{N+1} \frac{D_k}{v_k}. \tag{4.1}$$

The amplitude change along a ray is also computed assuming that a source of unit strength is located at $\mathbf{x}_S$. In a narrow tube of rays surrounding the ray in question it is assumed that the energy in the wave is conserved. Then the change in energy along the ray is proportional to the normal cross-sectional area of the ray-tube; that is, it is proportional to the Jacobian of the mapping induced by the rays. This is a purely geometrical effect and is called "geometric spreading". The computation of the geometric spreading factor, G, or equivalently of the Jacobian of the ray mapping from wavefronts at $\mathbf{x}_S$ to those at $\mathbf{x}_R$ is given by formulas in Červený et al. [1] or in Perozzi [5]. G depends on the curvature of the reflecting or refracting interface at each node on the ray, on the curvature of the wavefronts, on the distances between nodes, and on the ratio of propagation speeds on incident and transmitted or reflected signals. A derivation of the geometric spreading factor for rays from a point source incident on a curved interface is given in Keller and Keller [4].

In addition at each incidence of a ray upon an interface the ray splits, in general, into two reflected rays and two transmitted rays. The energy carried by an incident ray must be appropriately partitioned amongst the four rays it generates. This partition is determined by energy conservation and yields the reflection and transmission coefficients at each interface. These coefficients are computed by solving a linear system in four unknowns. This system is derived in H. B. Keller [2] and the computational details are summarized in Perozzi [5]. The amplitude factor E, for a given ray is simply the product of the appropriate reflection or transmission coefficients for each node on the ray.

The total amplitude change for a given ray is thus the product GE and we easily compute this factor for each ray by applying the formulas referred to above.

Finally we also compute the phase change along each ray. This data is required if we wish to produce continuous synthetic seismograms using standard convolution codes. There are three possible sources of phase change: i) reflections, ii) caustics, iii) critical or supercritical rays.

The reflections are easily detected and yield a phase change of: $\gamma_{\mathrm{i}} = \pi$ for a reflection and $\gamma_{\mathrm{i}} = 0$ for a transmission. At most one caustic occurs on each ray segment between adjacent nodes. The phase change is: $\gamma_{\mathrm{ii}} = \pi/2$ if a caustic occurs and $\gamma_{\mathrm{ii}} = 0$ if no caustic occurs. The occurrence of a caustic is automatically detected in the course of computing the contribution to the geometric spreading factor between two adjacent nodes (see Perozzi [5, pp. 31–33]). Supercritical rays occur when the linear system determining the reflection and transmission coefficients become complex (due to imaginary angles). The coefficients, α, in this case are of the form $\alpha = |\alpha| e^{i\phi}$ with $0 \leqq \phi < 2\pi$. Then the phase change is simply $\gamma_{\mathrm{iii}} = \phi$. The total phase change on the ray segment $[\mathbf{x}_{k-1}, \mathbf{x}_k]$ is thus

$$\gamma^k = \gamma_{\mathrm{i}}^k + \gamma_{\mathrm{ii}}^k + \gamma_{\mathrm{iii}}^k$$

and so the total phase change on a ray is

$$\gamma = \sum_{k=1}^{N} \gamma^k.$$

5. Example. The above indicated techniques have been employed in a variety of tests and examples, see Perozzi [5]. We present here a typical such example which also illustrates the fact that the rays of each class need not be unique or need not even exist. A complete existence and uniqueness theory for rays has never been developed although some modest beginnings are contained in Perozzi [5].

The geometry for this example is sketched in Fig. 2. The earth's surface and two interfaces are represented by the formulas:

a) $$y = f_0(x) \equiv 0,$$

b) $$y = f_1(x) \equiv x\left(\left(\frac{x}{10}\right)^2 - 1\right) - 5,$$

c) $$y = f_2(x) \equiv -10\left(\left(\frac{x}{10}\right)^2 + 1\right).$$

Five receivers are located at the points $\mathbf{x}_R^{(i)} = (i, 0)$, $i = 0, 1, \cdots, 4$. The top and bottom media are the same, denoted by index $m = 1$, and the middle medium is denoted by $m = 2$. The speeds in medium 1 are:

$$v_P \equiv v_2 = 2.44, \qquad v_S \equiv v_3 = 1.71;$$

and in medium 2 they are:

$$v_P = v_4 = 5.38, \qquad v_S = v_5 = 3.44.$$

All the rays in each of the seven families indicated in Fig. 3 yield a total of 292 rays.

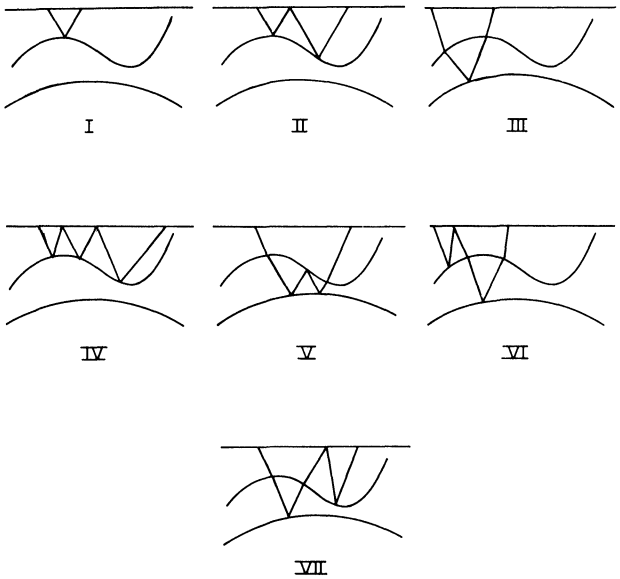

FIG. 3. *Seven families of rays for the three layer example. With* 2^{N+1} *rays in a family with N nodes there are* 292 *rays in all of the families shown.*

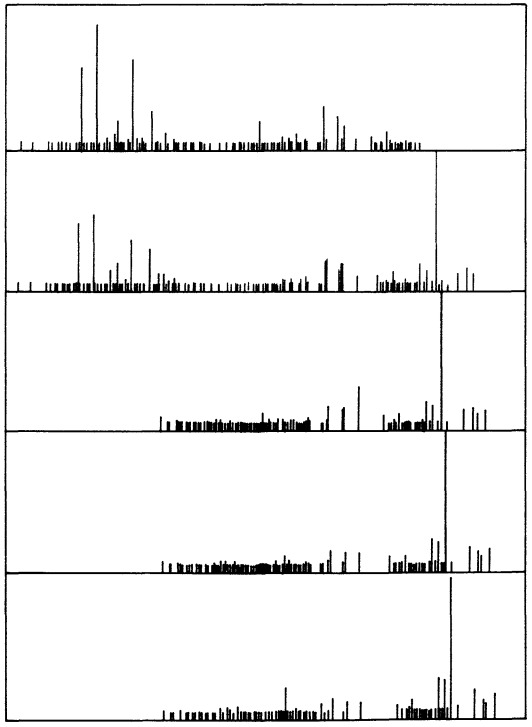

FIG. 4. *Amplitude* (log) vs. *arrival time for each of the five stations in the gather. This is the basic data from which artificial seismograms can be formed.*

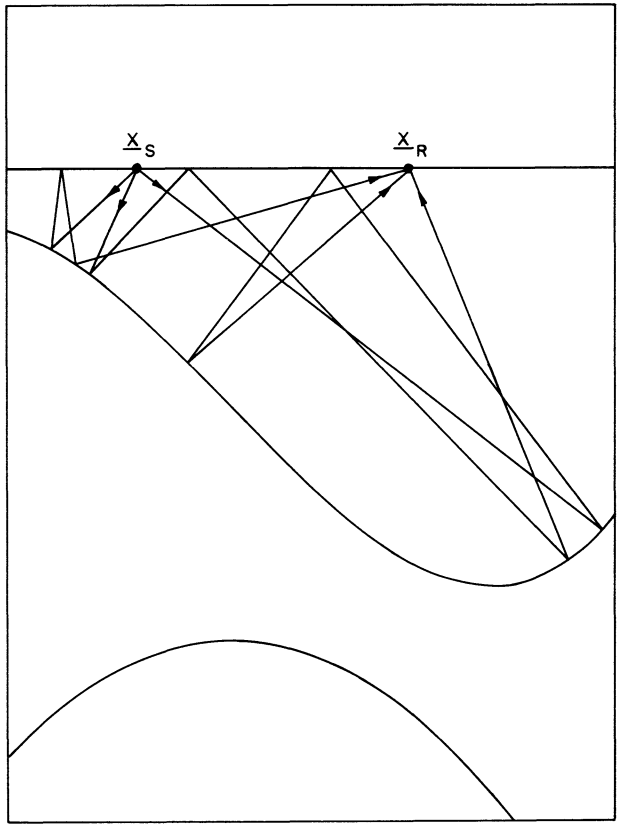

FIG. 5. *Nonunique rays of class* II. *Here three rays of type PPPP join* $\mathbf{x}_S = (-2, 0)$ *to* $\mathbf{x}_R = (4, 0)$.

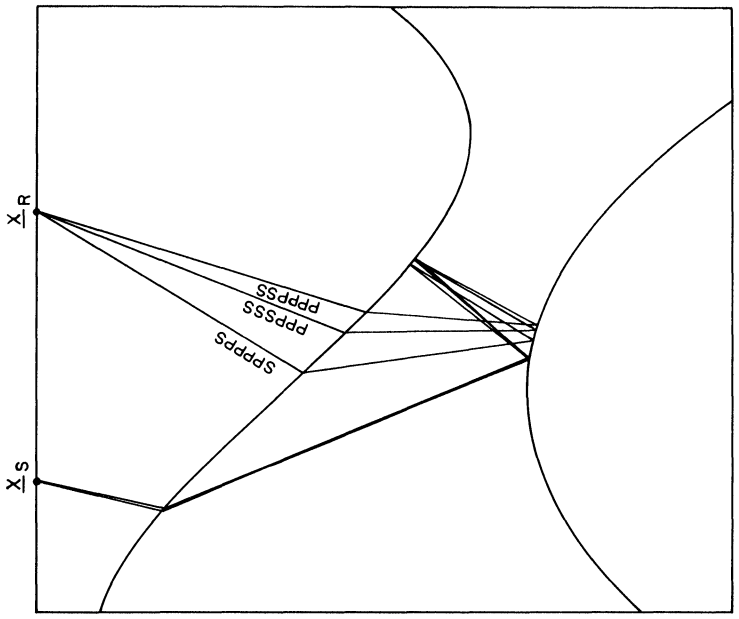

FIG. 7. *Three rays of class V. The initial speeds in the continuation leading to these rays contained negative values.*

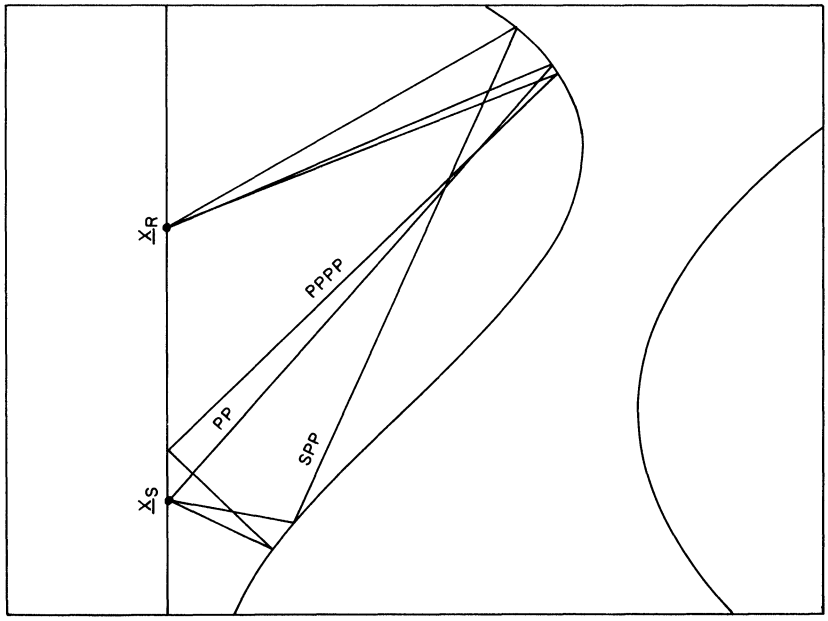

FIG. 6. *No ray of type PPP could be found joining* $\mathbf{x}_S$ *and* $\mathbf{x}_R$ *while types PP, SPP, and PPPP are shown. Note that the "missing" ray and the SPP ray are not in any of the ray classes of Fig.* 3.

In Fig. 4 we show the amplitudes against arrival times for 228 rays computed at each of the five stations in the gather indicated in Fig. 2. The seemingly equal amplitude of most of the low amplitude rays is merely due to scale difficulties. Two distinct structures are clearly indicated but more stations (or rays, or both) are required to refine their shapes. By convolving the signal responses of Fig. 4 with a typical seismometer response function artificial seismograms of reasonable resemblance to true ones are easily obtained.

In Figs. 5, 6, 7 we show some computed rays illustrating: nonuniqueness in Fig. 5 where three rays of class II (of type *PPPP*) are shown joining $\mathbf{x}_S = (-2, 0)$ to $\mathbf{x}_R = (4, 0)$; nonexistence in Fig. 6 where rays of types *PP*, *SPP*, *PPPP* are shown but no ray of type *PPP* could be found. Note that the *SPP* ray is not included in the classifications of Fig. 3. Finally in Fig. 7 three rays of class *V* (see Fig. 3) are shown. The initial speeds for the continuation leading to these rays contained some negative values but no difficulties result.

REFERENCES

[1] V. ČERVENÝ, I. A. MOLOTKOV AND I. PSENCIK, *Ray Method in Seismology*, Univerzita Karlova, Praha, 1977.

[2] H. B. KELLER, *Propagation of stress discontinuities in homogeneous elastic media*, SIAM Rev., 6 (1964), pp. 356–382.

[3] J. B. KELLER, *A geometrical theory of diffraction*, in Calculus of Variations and Its Applications, Proc. Symp. Applied Math., Vol. VIII, McGraw-Hill, New York, 1958, pp. 27–52.

[4] J. B. KELLER AND H. B. KELLER, *Determination of reflected and transmitted fields by geometrical optics*, J. Optical Soc. Amer., 40 (1950), pp. 48–52.

[5] D. J. PEROZZI, Ph.D. thesis, Part I. *Seismic ray-tracing in piecewise homogeneous media*, California Inst. of Technology, Pasadena, 1980, pp. 2–80.